https://doi.org/10.1016/j.engstruct.2017.09.049

Reinforcing strategies for double-coped beams against local web buckling

Cheng Fang[a]*, Michael C. H. Yam[b], Angus C. C. Lam[c], and Ke Ke[b]

[a)] *Department of Structural Engineering, School of Civil Engineering, Tongji University, Shanghai 200092, China*

[b)] *Department of Building & Real Estate, The Hong Kong Polytechnic University, Hung Hom, Kowloon, Hong Kong SAR, China*

[c)] *Department of Civil & Environmental Engineering, University of Macau, Macau SAR, China*

**Corresponding author: email: chengfang@tongji.edu.cn, Tel: +86 21 65982926*

Abstract: This paper presents a comprehensive numerical study on the strength and behaviour of double-coped beams (DCBs), with the focus on reinforcing strategies against local web buckling. Four reinforcement types, namely, longitudinal web stiffener (Type A), combined longitudinal and vertical web stiffeners (Type B), vertical and double longitudinal web stiffeners (Type C), and full-depth doubler plate (Type D), are considered. Through examining a suite of validated numerical models with a spectrum of cope details, it is found that the considered reinforcement types are in general effective, especially for the models with long or deep copes. Depending on the cope details and stiffener type, a series of failure modes, including local web buckling, web shear yielding, web shear buckling, tensile fracture of the bottom cope corner, and web crippling, are identified, and the effectiveness of the different reinforcement types on preventing or postponing these failure modes is discussed in detail. A preliminary design rule for checking the capacity of the reinforced coped section is also proposed in the paper, and additional analysis is performed to further evaluate the influences of varying reinforcement dimensions and boundary conditions on the ultimate capacity of the DCBs. Based on the numerical analysis, a set of prescriptive recommendations on reinforcement details is finally proposed, offering a simple yet safe guidance for new design or upgrade of DCB members.

Keywords: Double-coped beam; stiffener; doubler plate; local web buckling; numerical study; prescriptive design methods.

1. Introduction

In typical steel structures such as building frames, the flanges of secondary beams are often notched/coped in order to provide sufficient clearance for the connection zone and to facilitate the fabrication of flooring, decking, and ceiling systems. A beam is known as a single-coped beam (SCB) if part of the top flange is removed. When both flanges need to be partially removed at the beam ends according to certain construction or structural requirements, the beam is called a double-coped beam (DCB), as shown in Fig. 1(a). For both cases, the strength of the coped end is inevitably compromised, and as a result, these members may experience complex failure modes, including local web buckling [1-3], block shear [4-8], fatigue fracture [9-11], and lateral-torsional buckling [12-13]. Local web buckling, a phenomenon caused by local instability of the compressive coped edge, is one of the most common local failure modes for both SCBs and DCBs [14]. The failure mechanism was investigated by a number of researchers, leading to the stipulation of design equations in the AISC Steel Construction Manual [15] and SCI design guidelines [16]. With continuously emerging test and numerical data, some further amendments to the existing design rules were also suggested [3, 17-18].

Recognising the detrimental effects caused by the copes, a series of reinforcing strategies with various stiffener types were proposed for SCBs. Cheng et al. [1] numerically examined the effectiveness of three types of stiffeners, namely, longitudinal web stiffener, combined longitudinal and vertical web stiffeners, and doubler plate, on the local web buckling capacity of SCBs. The details of these stiffeners are reproduced in Fig. 1(b). It was claimed that the longitudinal stiffener and doubler plate reinforcement types were suitable for standard hot-rolled steel sections. In the case of slender webs, i.e. thin web members with $D/t_w > 60$ (D = Full beam depth, t_w = web thickness), combined longitudinal and vertical stiffeners might need to be employed. Yam et al. [19-21] later confirmed the benefits of these stiffeners via an experimental study, and it was found that the combined longitudinal and vertical stiffeners could effectively prevent web crippling near the end-of-cope section (position of the section is defined in Fig. 1(a)), and thus were recommended for the case of deep copes. The subsequent parametric study revealed that SCBs reinforced by

longitudinal or combined longitudinal and vertical stiffeners were able to develop either the plastic moment capacity of the full beam section or the shear yield capacity of the coped section, but it should be noted that this conclusion was made based on models with a fixed beam span (i.e. 2m) under a single concentrated load. In addition, using two vertical stiffeners was suggested for very slender beam sections such as built-up girders. Some of the afore-mentioned reinforcement types have been included in the AISC Steel Construction Manual [15].

While the existing studies clearly demonstrated the beneficial effects of the various reinforcing strategies for coped beams, these results were obtained based on the research data related to SCBs. So far, relevant information on reinforced DCBs is very rare. Some investigations warned that due to the absence of the restraint from both flanges, DCBs can exhibit much weaker local web buckling performance compared with the case of SCBs [22-23]. In addition, as the reinforced DCBs may have different behaviour from reinforced SCBs, the applicability of the existing reinforcing strategies to DCBs is still unclear. These facts highlight the necessity of understanding the strength and behaviour of reinforced DCBs, such that effective reinforcing strategies can be proposed to support new design or retrofitting of such members. To this end, an experimental study [24] was recently performed by the authors and co-workers of this paper. The results indicated that some of the existing reinforcing strategies (for SCBs) may also be effective for DCBs against local web buckling, but meanwhile, new failure modes were observed which need extra attention.

This study is an extension of the previous experimental programme [24] to acquire more in-depth understanding of the performance of reinforced DCBs. In this paper, the general information on the tests and the key results are briefly introduced, and the corresponding detailed Finite Element (FE) analysis on the test specimens are performed. The influence of initial imperfection magnitude is also discussed. After achieving satisfactory agreement between the test results and the FE predictions, a further parametric study is performed exploring the influence of various parameters, including coping dimension, reinforcement types and dimensions, and boundary conditions, on the

strength and behaviour of DCBs. Based on the results from the parametric study, a set of design recommendations is finally proposed.

2. Modelling approach and validation

2.1 *Tests conducted by Lam and colleagues [24]*

Eight full-scale DCB specimens were tested in the research programme by the authors and his co-worker [24]. The specimens were made from S355 UB406×140×39 steel beams. Two coping dimensions, i.e. c = 450 mm (d_c = 25 mm) and c = 550 mm (d_c = 50 mm), were considered as illustrated in Fig. 2 and Table 1. For each coping dimension, one specimen was unreinforced (UR) and the remaining three were strengthened with varied reinforcement types, namely, longitudinal web stiffener (LWS), full-depth doubler plate (FDP), and partial-depth doubler plate (PDP). The longitudinal web stiffeners were fillet welded along the top edge of the coped web on both sides of the web, and the doubler plate was welded on one side of the coped web. The extension of the stiffener or doubler plate (e_x, Fig.2) was 50 mm and 100 mm for C450 and C550 series specimens, respectively. For the case of PDP, the plate depth was half of the coped web depth. Flush end-plate connections were adopted at the coped end for all the specimens. A simply-supported condition was arranged for the test beam, where the coped end was supported by the reaction frame via the end-plate connection. The far end of the beam was placed on a roller support. The loading condition of the test beam is schematically shown in Fig. 2. Lateral-torsional buckling of the test beam was prevented by out-of-plane restraints provided to the flanges of the beam close to the loading point and the end supports.

According to the test results, local web buckling governed the final failure mode for the two unreinforced specimens. Adding a pair of longitudinal web stiffeners eliminated local web buckling, but tensile cracking at the bottom cope corner was finally developed. Employing a doubler plate could delay the occurrence of local web buckling, and a full-depth doubler plate seemed to be more effective than a partial-depth one. In addition, the cope details were shown to influence the local web buckling capacity of DCBs. The key test results, including the ultimate load P_{test}, ultimate

reaction at the coped end R_{test}, and the failure mode, are reproduced in Table 1. More detailed information can be found in [24].

2.2 Modelling approach

The test results were used to validate the finite element (FE) models. The general FE programme ABAQUS [25] was adopted for simulating the test specimens, and both geometric and material nonlinearities can be captured. Four-node shell elements with reduced integration, i.e. S4R elements in ABAQUS nomenclature, were used to mesh the structural members with a mesh size of approximately 10 mm. The measured dimensions of the specimens were used in the models. For the shell elements simulating the doubler plate, a shift of the reference plane was made, such that the single-sided reinforcing condition could be reasonably reflected. As weld failure was not considered in the current study, the welds between members and components were simulated via a 'tie' interaction. The boundary conditions, including the lateral restraints, were appropriately defined such that the actual testing conditions were sufficiently reflected. An overview of the typical model and the associated boundary conditions are illustrated in Fig. 3(a).

The nonlinear material properties of steel were characterized by an isotropic hardening model with an idealised multi-linear stress-strain response and the von Mises yield criterion. The key material properties, including the Young's modulus, yield strength, ultimate strength, and fracture strain, were taken from the tension coupon test results, as reproduced in Table 2. In particular, the possible fracture behaviour of the web panel was taken into account by introducing a ductile damage criterion [25], where the fracture progress was controlled by a damage initiation criterion and a damage evolution law. The damage initiation criterion describes the maximum strain which initiates damage, i.e. the starting point of the decreasing branch of the stress-strain curve. This strain causes material stiffness degradation, where the value can be obtained from a material test. The damage evolution law describes the rate of degradation of the material stiffness once the corresponding initiation criterion has been reached. This rate often has no significant effect on the ultimate load, but may affect the load decreasing response after ultimate load. In the current model,

a linear damage evolution law was considered, and a sufficiently large damage displacement (i.e. 1 mm) was taken for numerical stability [26]. Adopting this method, the material stiffness starts to degrade when the damage initiation strain is reached, and the stiffness decreases linearly until complete loss of the strength and stiffness of the damaged elements.

The FE analysis involved an elastic buckling analysis (eigenvalue analysis) and subsequently a nonlinear load-deflection analysis. The initial imperfection of the specimens was represented according to the fundamental buckling mode of the model obtained from the elastic buckling analysis. With such initial imperfection shape and an appropriate imperfection magnitude, the nonlinear load-deflection analysis was carried out to capture the nonlinear responses of the models with increasing load. The imperfection magnitude can be scaled to any desirable value to cater for imperfection sensitivity analysis. EN1993-1-5 [27] suggests that for buckling analysis of plated structures, the imperfection magnitude could be taken in proportion to the length of the considered panel. Since the actual imperfection conditions were not measured in the test programme, three levels of initial imperfection magnitude, namely, $c/1000$, $c/200$, and $c/100$ (where c is the cope length) were considered in the validation study.

2.3 Model validation

The deformation and failure behaviour of the FE models agree well with the test observations, as shown in Fig. 3(b). In particular, the buckling line, yield pattern, and fracture response of the coped region are adequately captured. The predicted load-deflection curves of the specimens also show satisfactory agreement with the test results, as shown in Fig. 4(a). Minor discrepancies are found in some models at the load descending stages (e.g. C450dc25-UR), but the overall trend of the nonlinear load-deflection responses are sufficiently reflected. The initial imperfection magnitude seems to have minor to moderate influences on the ultimate load of the models. Negligible imperfection sensitivity is exhibited for the models with longitudinal stiffeners since these models failed in tensile fracture of the bottom cope corner. The unreinforced models, which fail in local web buckling, also show limited imperfection sensitivity. This phenomenon is

attributed to the development of stable post-buckling resistance in thin coped webs. The post-buckling mechanism has been confirmed by a previous study on unreinforced DCBs and the detailed discussion can be found in [23]. When the coped web is reinforced by a doubler plate, the models also fail in local web buckling, although the occurrence of the failure is delayed. With the added thickness of the web (due to the presence of the double plate), the stable post-buckling behaviour is suppressed, and an increased level of imperfection sensitivity is exhibited. The ultimate loads (P_{FE}) of the models with varying imperfections are shown in Table 1. It is observed that an imperfection of $c/200$ leads to a mean P_{FE}/P_{test} ratio of 1.0 and a sufficiently low level of CoV (coefficient of variation). Therefore, this imperfection magnitude may be consistently used in the following parametric study.

In order to examine the mesh dependency, two extra mesh sizes, 5 mm and 20 mm, were used in C450dc25 series models that exhibit two typical failure modes, i.e., local web buckling and cope corner fracture. As shown in Fig. 4(b), models C450dc25-UR, C450dc25-FDP, and C450dc25-PDP are not very sensitive to the mesh size, whereas model C450dc25-LWS exhibits certain sensitivity (although not significant). This indicates that the fracture resistance slightly depends on the mesh size. Considering 10 mm mesh size as the reference case, the deviation of ultimate load is typically within 5% when the other mesh sizes are used. Nevertheless, it is believed that a 10 mm mesh size could lead to a reasonable balance between accuracy and computational efficiency.

The FE models could be further validated through comparing the strain responses between the test and FE results. Fig. 5 shows the typical longitudinal strain distributions over the end-of-cope section. The calculated strain distribution, which is based on $M_{co}y/I_{co}$ (M_{co} is the moment applied at the end-of-cope section, y = distance between the point of interest and the neutral axis, I_{co} is the second moment of area of the end-of-cope section), is also shown in the figure. For the reinforced specimens, the cross-sectional properties (e.g. I_{co}) were calculated using an equivalent cross-section taking account of both the coped web and the stiffener or doubler plate. Reasonable

agreement is generally observed between the FE and test results. The discrepancies could be caused by the geometrical imperfections of the test specimens. More specifically, due to possible minor out-of-plane plate bending action over the coped web panel at the initial loading stage, the readings from the strain gauges mounted at one side of the web plate can differ from the strains extracted from the middle reference plane of the shell elements in the FE models. Satisfactory agreement is also observed between the FE and calculated results, although the stress concentration effect, which is not considered in the calculated strains, may cause a certain level of discrepancy.

3. Parametric study

3.1 Parameter matrix

Having shown that good agreement exists between the FE and test results, a further parametric study was conducted to examine the influence of varying reinforcing strategies on DCBs with a spectrum of cope details. According to the failure modes revealed by the available test and FE results, four reinforcement types were considered, namely, longitudinal web stiffener (Type A), combined longitudinal and vertical web stiffeners (Type B), vertical and double longitudinal web stiffeners (Type C), and full-depth doubler plate (Type D), as shown in Fig. 2. The thicknesses of the stiffeners (longitudinal and vertical) and the doubler plate were considered to be the same as those of the flange and the web, respectively. For each reinforcement type, a fixed stiffener extension, i.e. $e_x = d_c$ and $e_y = d_c$ (symbols are illustrated in Fig. 2), was considered. In addition, the lateral displacement of the top flange was restrained, a case which can be practical for composite beams or other conditions where lateral-torsional buckling is prevented. Further discussions are made on the influences of different extension dimensions and boundary conditions on the strength and behaviour of DCBs, as will be presented later in Section 4.

A representative S355 UB406×140×39 steel beam was adopted for the parametric study. For consistency of the analysis, the modelling approach as well as the loading and boundary conditions were identical to those discussed in the validation study. It should be noted that the UB406×140×39 section has the largest d/t_w ratio (d is the effective depth of web between the two fillets, and t_w is

web thickness) among the available hot-rolled universal beams, and it is believed that the discussions and conclusions made in this paper could be safely applied to other sections. A set of material parameters, conforming to the Eurocode 3 recommendation [28], was consistently taken for all the models, i.e. Young's modulus E = 205 GPa, yield strength f_y = 355 MPa, ultimate strength f_u = 510 MPa, and strain at fracture ε_u = 0.20. In order to cover most of the practical dimensions of the copes, the considered cope length-to-beam depth ratio (c/D) ranged from 0.2 to 1.4 (80 mm to 438 mm), and the cope depth-to-beam depth ratio (d_c/D) varied from 0.05 to 0.25 (20 mm to 100 mm), leading to a total of 60 basic models being built, as shown in Table 3. For easy reference, each model was designated with a model code, starting with the c/D ratio, followed by the d_c/D ratio, and ending with the reinforcement type, e.g. C0.8dc0.15-A. The typical geometric configurations and key symbols of the models are shown in Fig. 2.

3.2 General failure response

A variety of local failure modes, including local web buckling, web shear yielding, web shear buckling, tensile fracture of the bottom cope corner, and web crippling, are observed for the models, as typically shown in Fig. 6. In some cases, one failure mode occurs first and then followed by the other one, e.g. web crippling followed by tensile fracture for some models with Type A reinforcement. The failure mode is strongly dependent on the cope dimension and stiffener type. Local web buckling is the governing failure mode for the unreinforced models with a cope length being equal to or greater than 0.5c. Local web buckling also tends to occur in the models reinforced with a doubler plate (Type D) and concurrently with a relatively long cope, e.g. model C0.8dc0.05-D. For the case of short cope, i.e. c/D = 0.2, the models generally failed in shear yielding through the depth of the coped web, and it seems that the failure mode is not influenced by the presence of the longitudinal and vertical stiffeners which have limited contribution to the shear resistance. When no reinforcement is employed, the shear yielding of the coped web is often followed by local web buckling at late loading stages.

Tensile fracture of the bottom cope corner is the most common failure mode for the models with Type A or Type B reinforcement. The upshifting of the neutral axis (due to the presence of the top horizontal stiffeners), accompanied by stress concentration effect, attributes to a significantly increased tensile stress level at the bottom cope corner. Adding an extra pair of longitudinal stiffeners along the bottom cope edge (Type C) can help reduce the stress level, although for some models, i.e. those with $c/D \geq 0.8$, fracture can still occur at the web near the tip of the bottom longitudinal stiffener adjacent to the cope corner. Nevertheless, the tensile cracking resistance is effectively increased when Type C reinforcement is employed. Another common failure mode is web crippling, which occurs in Type A and Type D reinforced models with a relatively deep cope depth, i.e. $d_c/D \geq 0.15$. This type of failure is caused by local instability of the web above the top cope edge, and is often accompanied by lateral displacement of the longitudinal stiffener or doubler plate, as shown in Fig. 6. Adding vertical stiffeners (i.e. Types B and C) could effectively prevent web crippling. Web shear buckling is a special failure mode occurring in Type C reinforced models only, e.g. model C0.5dc0.15-C. This failure mode is caused by the high shear action applied over the slender coped web panel.

3.3 Load-deflection response

The typical load-deflection responses of the models are shown in Fig. 7. In order to highlight the local deformation condition of the coped region, the vertical displacement of the end-of-cope section (δ_l) is presented as the abscissa in the figure. It should be noted that the top flange of the beam was considered for δ_l measurement such that the possible web crippling effect can be reflected. The curves generally show a linear response at the beginning of loading, and subsequently there is a nonlinear load ascending stage prior to reaching the ultimate load. This nonlinear ascending stage varies significantly in different models due to different load resisting mechanisms. For the models with a short cope (C0.2 series) and equipped with Type A, B or C reinforcement, the increase of the load at the nonlinear stage is related to evident shear yielding of the coped web. For the unreinforced one, the web shear yielding is followed by local web buckling. When a doubler

plate is considered (Type D), the ultimate load is achieved upon the occurrence of web crippling. Similar load-deflection responses are shown for the C0.5dc0.15 series models, but no such shear yielding is developed in the unreinforced model due to early local web buckling. In addition, the web shear yielding of Types A-C reinforced models was terminated by either tensile cracking or web shear buckling. With further increases of the cope length, i.e. C0.8dc0.15 and C1.1dc0.15 series models, the ultimate load of the reinforced models is achieved upon tensile cracking or web crippling, and again, the load resistance of the unreinforced models starts to drop soon after the occurrence of local web buckling.

In general, compared with the unreinforced models, Types A to C reinforcements could lead to the increase of both the ultimate load and the corresponding deformation capacity. The deformation of the coped region at ultimate load for these reinforced models is often larger than 10 mm. Type D reinforcement can effectively increase the ultimate load, but is less effective in increasing the deformation capacity due to web crippling. In other words, the instability type failure modes, including local web buckling and web crippling, lead to much less deformation capacity of the coped region than the strength type failure modes (i.e. shear yielding and tensile fracture). After achieving the ultimate load, the load decreases gradually.

3.4 Effectiveness of reinforcement

The effectiveness of the reinforcing strategies can be evaluated by examining the ultimate coped end reactions (R_u) of the models with different reinforcing details. The normalised R_u (i.e. normalised by the value of the unreinforced case) is given in Fig. 8(a). The results demonstrate that for the current suite of models, R_u can be increased to up to 4.5 times of that of the corresponding unreinforced ones due to the presence of the reinforcement, however, an evident variation of the effectiveness of different reinforcement types is observed. The stiffeners and doubler plates, which help prevent or delay local web buckling, are more effective for the models with longer and deeper copes. When the unreinforced models failed in web shear yielding, i.e. C0.2 series models, the benefit of the longitudinal and vertical stiffeners is limited due to their negligible contribution to

section shear resistance. Although using a doubler plate could effectively increase the shear yielding resistance of the coped section, the actual increase of R_u is still limited for the C0.2 series models. This is due to the occurrence of other failure modes (e.g. web crippling) that prohibited a full utilisation of the shear yielding capacity of the strengthened web. Generally speaking, among the four reinforcing strategies, Type C reinforcement leads to the most significant increase of R_u. A similar level of effectiveness is offered by Types A and B reinforcements, although different failure modes often occur in these two cases. Less benefit is provided by Type D reinforcement, where the corresponding reinforced models are up to 2.5 times the R_u of the unreinforced ones.

From a section utilisation point of view, the behaviour of the coped section could be alternatively interpreted by $R_u/R_{y,co}$, $R_u/R_{p,co}$, and $R_u/R_{vy,co}$ ratios, as shown in Fig. 8(b) through 8(d). $R_{y,co}$ is the reaction where first flexural yielding of the coped section (including reinforcement) is achieved, and it can be calculated by $R_{y,co} = M_{y,co}/c$, where $M_{y,co}$ is the theoretical elastic moment capacity of the coped section, and c is the cope length; similarly, $R_{p,co}$ is the reaction where the theoretical plastic moment capacity of the coped section is achieved. In addition, the shear capacity ($R_{vy,co}$) of the coped section can be obtained by $R_{vy,co} = f_y A_w / \sqrt{3}$, where f_y is yield strength, and A_w is shear resisting area of the cross section. For reinforced coped sections, the cross-sectional properties (e.g. second moment of area and shear resisting area) were calculated based on equivalent cross-sections including the stiffeners or doubler plate.

The results show that the moment capacity of the coped section can be better mobilised for the models with deeper copes. The cope length can also slightly influence the $R_u/R_{y,co}$ and $R_u/R_{p,co}$ ratios. For most of the unreinforced models, $R_{y,co}$ can be achieved, but local web buckling prevents the coped section from advancing into $R_{p,co}$. Types A and B reinforcements could lead to a full utilisation of the elastic moment capacity of the reinforced coped section, but approximately half of these models failed to achieve $R_{p,co}$ due to web crippling or tensile fracture. It is difficult for Type C reinforced models to reach either $R_{y,co}$ or $R_{p,co}$, because of the high stresses concentrated near the tip of the longitudinal stiffeners, causing fracture of the beam web. When Type D reinforcement is

considered, the majority of the models could reach $R_{y,co}$, among these models only few could allow a full utilisation of the plastic moment capacity of the reinforced coped section. The results shown in Fig. 8(d) confirm that most of the C0.2 series models, with the $R_u/R_{vy,co}$ ratios being above unity, mainly fail in web shear yielding. For most models with longer copes, $R_{vy,co}$ is not reached due to the occurrence of other failure modes prior to web shear yielding.

4. Further discussions

4.1 Influence of reinforcement extension

In the above-mentioned basic models, the stiffener or doubler plate extensions were equal to the cope depth. As a further expansion of the parameter matrix, the influence of the reinforcement dimension is investigated. The ultimate reactions (R_u) of typical models with varying stiffener or doubler plate extensions are given in Figs. 9(a) through 9(e). It should be noted that these representative models were particularly selected, according to their failure modes, to highlight the potential influence of the reinforcement dimensions. For ease of comparison, the R_u values of the corresponding unreinforced models are also given in the figures. As shown in Fig. 9(a), the extension (e_x) of Type A longitudinal web stiffeners has a moderate influence on R_u, where the value is on average increased by 30.8% for the considered two model series when e_x is increased from 0 mm to 100 mm. Local web buckling of the unreinforced model is effectively prevented by the stiffeners even with e_x = 0 mm, but local web crushing or web crippling can be developed instead. With increasing e_x, tensile fracture of the bottom cope corner starts to govern the failure mode, and a further increase of e_x would provide limited benefit. This explains the slower rate of increase of R_u for model C0.8dc0.05-A when e_x is larger than 40 mm as shown in Fig. 9(a).

Type B reinforcement is mainly used for preventing early web crippling. The influence of the vertical stiffener extension (e_y) is shown in Fig. 9(b) ($e_x = d_c$). It is clearly observed that compared with the unreinforced case, R_u is significantly increased by the vertical stiffeners, but the influence of the stiffener extension is very limited. For all the models with varying e_y, the failure mode is tensile fracture of the bottom cope corner. The FE results indicate that the segment between

the top flange and the longitudinal stiffener is sufficient for preventing web crippling, whereas the vertical stiffener extension offers little benefit. For Type C reinforcement, the influence of the extension (e_x) of the lower horizontal stiffener on R_u is shown in Fig. 9(c) ($e_x = d_c$ and $e_y = d_c$ for the upper horizontal and vertical stiffeners). It is observed that when e_x is increased from 0 mm to 100 mm, R_u is on average increased by 58.5%. The failure mode of these models is tensile fracture of the web near the tip of the lower horizontal stiffeners, but increasing e_x could delay the initiation of fracture. Another important finding, through comparisons between Fig. 9(c) and Fig. 9(b), is that when the coped beam models were strengthened by Type C reinforcement with e_x = 0 mm for the lower horizontal stiffener, the models exhibited even lower R_u than the models with Type B reinforcement. This indicates that the horizontal stiffener with no extension may cause a less favourable stress state at the bottom cope corner. This phenomenon suggests that a sufficient e_x should be employed for the lower horizontal stiffener if one wants to effectively delay tensile cracking by using Type C reinforcement. Further experimental studies may be needed to confirm this finding.

For the case of Type D reinforcement, the R_u of the models with a variation of doubler plate horizontal extensions (e_x) and vertical depths (e_y) are shown in Figs. 9(d) and 9(e), respectively. Compared with the unreinforced models, adding a doubler plate increases R_u to a certain extent. The reinforced models generally fail in web crippling accompanied by local web buckling, and the increase of e_x could delay the occurrence of the failure and thus leads to higher R_u. The value of R_u of the models with e_x = 100 mm is on average 58.7% higher than the case of e_x = 0 mm. Increasing the doubler plate depth (e_y) is also shown to benefit the ultimate reaction, noting that the same trend was observed in the experimental study [24]. The fundamental role that a doubler plate plays is to increase the local web buckling capacity of the coped region. It is found that with increasing e_y, the failure mode of the models starts to change from local web buckling to web crippling, and R_u is on average increased by 22.7% when e_y is increased from a quarter of the coped section depth to full depth.

4.2 Influence of lateral bracing

For the basic models, the lateral displacement of the beam's top flange is fully restrained. In practice, however, the beams may not be braced laterally, e.g. bare steel beams. In order to examine the behaviour of the reinforced DCBs with various bracing conditions, two additional cases, i.e. Case 1 and Case 2 bracing conditions, are assumed in selected models (i.e. C0.5dc0.15 and C0.8dc0.15 series). It is assumed in Case 1 that the lateral bracings of the beam top flange were removed, except for the load application point which represents a member junction where the local lateral restraint offered by the intersecting beams could exist. For Case 2, the local lateral restraint at the load application point is further removed, such that the entire length of the beam flange is free to displace laterally. The continuous lateral bracing condition considered in the basic models is named as the 'reference case' in the following discussion. It is noted that for the two additional cases, the same geometric imperfection configuration as that considered in the reference case is used for consistency.

As indicated in Fig. 10(a), the ultimate reactions of the unreinforced models with the Case 1 lateral bracing condition are slightly lower than those of the reference models, but generally speaking, the two cases lead to comparable local web buckling resistance. A similar finding was reported in [23] where Case 1 led to an approximately 10% decrease of R_u compared with the reference case for DCBs with a spectrum of cope details. When the models are equipped with Type A through Type C reinforcements, the reference and Case 1 bracing conditions result in negligible differences in terms of R_u, and the failure mode is also unaffected. This indicates that the three reinforcing strategies are also highly effective for Case 1 bracing conditions. For the models with Type D reinforcement, the Case 1 bracing condition results in an approximately 20% decrease of R_u compared with the reference case, and this is due to the fact that the absence of the lateral restraint immediately near the end-of-cope section decreases the load resistance against web crippling.

On the other hand, the unreinforced models (UR) with the Case 2 bracing condition show significantly lower resistance when compared with either the reference or Case 1 models. Evident

lateral displacement of the beam top flange (i.e. lateral torsional buckling) is observed in the Case 2 models. This indicates that a complete removal of the lateral bracing along the entire beam length considerably increases the risk of lateral torsional buckling for unreinforced DCBs. Type A through Type C reinforcements are shown to effectively prevent the lateral displacement of the beam flange near the end-of-cope section, and the resulting ultimate reactions are comparable to those obtained from the reference or Case 1 bracing condition. For the models with Type D reinforcement, the Case 2 bracing condition leads to lateral torsional buckling failure, and results in a 40%-50% decrease of R_u compared with the reference case. Summarizing the above findings, it can be concluded that the ultimate reactions of unreinforced DCBs do depend on the lateral bracing condition of the beam, but this dependence becomes insignificant when Type A through Type C reinforcements are adopted. In other words, the three reinforcement types can all effectively increase the ultimate reaction, regardless of the lateral bracing condition for the coped details examined. Type D reinforcement is less effective in preventing local web buckling and lateral torsional buckling, especially for the Case 2 bracing conditions, as the doubler plate plays a limited role in preventing lateral displacement of the unrestrained beam top flange.

4.3 Influence of connection rotational stiffness

In practice, the connection rotational/bending stiffness can vary with different connection details. For the current study, the end-plate thickness is 10 mm, resulting in a calculated rotational stiffness of 452 kNm/rad (based on a FE analysis) for the connection. In order to examine the sensitivity of the DCB behaviour to connection stiffness, two extra cases were additionally considered, namely, idealised pin (free to rotate) and double end-plate thickness (20 mm). The latter leads to a connection rotational stiffness of 2884 kNm/rad, which may represent a typical semi-rigid connection behaviour. As shown in Fig. 10(b), an increase of connection rotational stiffness can increase the load carrying capacity of both the unreinforced and reinforced DCBs. This is because that a negative bending moment can be induced at the coped region with an increase in connection stiffness, and this effect tends to decrease the ‘effective buckling length’ along the top cope edge

and as a result changes the behaviour of local web buckling or other failure modes. One exception is model C0.5dc1.5-C, where the connection rotational stiffness has limited influence on the ultimate reaction. This is because that this particular model fails in web shear buckling which is not sensitive to the bending behaviour of the connection. The results generally indicate that Types A through D reinforcement can all effectively increase the ultimate reaction, regardless of the connection stiffness. The trend with varying reinforcement types seems to be similar for the models with different levels of rotational stiffness.

5. Design considerations

As mentioned, the recommended reinforcement details in AISC Steel Construction Manual [15] are based on an early numerical study conducted by Cheng et al. [1] with the focus on SCBs. Currently, there is no such recommendation available for DCBs. In addition, there is no design rule for checking the local capacity of the reinforced coped sections. With the newly obtained test and numerical data pool for DCBs, some design recommendations on 1) local section capacity evaluation and 2) practical reinforcing strategies, are proposed in this paper.

5.1 Reinforced coped section design

In practical design, the section capacity of a member is normally adequately evaluated via yield checking, provided that no local instability is expected. For DCBs, however, regular flexural and shear yield checking of the reinforced coped section may be unsafe, attributing to complex failure modes of the section (as discussed in detail in Section 3). This can be confirmed in Fig. 11(a) (the data are directly reproduced from Fig. 8(b) and 8(d)), where the ratios of the ultimate reaction R_u over minimum ($R_{y,co}$, $R_{vy,co}$) could be evidently below unity for a number of models, especially for those with Types C and D reinforcement. In light of this, reduction factors may be used for the yielding capacities of the reinforced coped sections, and in such a simplified way, the local coped section capacity (i.e. ultimate reaction) could be safely predicted by only checking two items: 1) flexural yielding capacity $\varphi_y R_{y,co}$, and 2) shear yielding capacity $\varphi_{vy} R_{vy,co}$, where the lower value governs.

As indicated by Fig. 11(a), conducting regular flexural yield ($R_{y,co}$) and shear yield ($R_{vy,co}$) checking seems to be safe for Types A and B reinforced coped sections, and therefore no reduction factor is required. For Type C reinforcement, it is suggested, according to current FE results, that a reduction factor of $\varphi_y = 0.8$ may be used for $R_{y,co}$, whereas no reduction is required for $R_{vy,co}$. Again, the lower value of $\varphi_y R_{y,co}$ and $R_{vy,co}$ governs the design. Similarly, for the case of Type D reinforcement, reduction factors of $\varphi_y = 0.9$ and $\varphi_{vy} = 0.5$ are suggested for $R_{y,co}$ and $R_{vy,co}$, respectively. As can be observed in Fig. 11(b), the ratios of R_u over minimum ($\varphi_y R_{y,co}$, $\varphi_{vy} R_{vy,co}$) are close to or above unity, indicating safe design. It should be noted that the prediction can be overly conservative for certain cases when the above design approach is considered. Finally, for the unreinforced (UR) coped sections, regular yield checking also tends to be safe, and therefore no reduction factor is necessary. Alternatively, a more advanced design approach has been proposed by the authors and co-workers for unreinforced DCBs, as detailed in [23].

5.2 Prescriptive recommendations on reinforcement details

Although the reinforcing target may vary with different design requirements, it is often desired that local failure of the coped region happens after the development of plastic moment capacity of the full beam section ($M_{p,b}$) or shear yielding capacity of the coped section ($V_{y,co}$). It is noted that the necessity of adopting reinforcement also strongly depends on the geometric configuration of the beam (e.g. span) and the load pattern (e.g. location and distribution of the load).

Considering the above, a typical S355 UB406×140×39 simply supported steel beam is used for the illustration of the reinforcement proposal. A typical span-to-depth (L/D) ratio of 10 was assumed for the steel beam. Larger L/D ratios, leading to easier development of $M_{p,b}$, would make the proposed reinforcement details (based on $L/D = 10$) conservative. Concentrated loads are assumed to be applied on the beams, and three load positions, with the shear spans (a) of $L/8$, $L/4$, and $L/2$, were considered. These may well cover the practical structural beam layouts encountered in a steel frame. For each beam with a particular load position, the maximum design support reaction, $R_{d,max}$, can be calculated based on $M_{p,b}$ and $V_{y,co}$, where the lower value governs. The

ultimate load (R_u) predicted by the FE models are compared with $R_{d,max}$, as shown in Fig. 12. A $R_u/R_{d,max}$ ratio being greater than unity indicates that the reinforcement is adequately effective in strengthening DCBs to develop the section capacity (either $M_{p,b}$ or $V_{y,co}$). According to the limited data from the parametric study as shown in Fig. 12, the following prescriptive reinforcing strategies are recommended for strengthening DCBs:

- Shear span = $L/8$. For copes with $c/D \leq 0.2$ and $d_c/D \leq 0.25$, no reinforcement is needed; for copes with $0.2 < c/D \leq 0.5$ and $d_c/D \leq 0.25$, Type C reinforcement is recommended. Types A, B, or D reinforcement can be alternatively employed, but only up to 90% of $R_{d,max}$ can be achieved; for copes with $0.5 < c/D \leq 0.8$ and $d_c/D \leq 0.25$, none of the considered reinforcement can fully mobilise the section capacity, but Type C reinforcement is the most effective one being able to achieve 80% of $R_{d,max}$; similarly, for copes with $0.8 < c/D \leq 1.1$ and $d_c/D \leq 0.25$, Type C reinforcement is the most effective one allowing at least 60% of $R_{d,max}$ to be achieved.
- Shear span = $L/4$. For copes with $c/D \leq 0.2$ and $d_c/D \leq 0.25$, or $0.2 < c/D \leq 0.5$ and $d_c/D \leq 0.05$, no reinforcement is needed; for copes with $0.2 < c/D \leq 0.5$ and $0.05 < d_c/D \leq 0.25$, Types A, B, or D reinforcement is recommended; for copes with $0.5 < c/D \leq 0.8$ and $d_c/D \leq 0.15$, Types A, B or D reinforcement can be used, while for $0.15 < d_c/D \leq 0.25$, Type C reinforcement is recommended; for copes with $0.8 < c/D \leq 1.1$ and $d_c/D \leq 0.15$, Type C reinforcement is recommended, but for $0.15 < d_c/D \leq 0.25$, Type C reinforcement can only lead to 80% of $R_{d,max}$. These recommendations can also be applicable to the case of uniform distributed load (UDL) pattern as the two load cases ($a = L/4$ and UDL) lead to the same relationship between the reaction and the mid-span moment, and thus the same $R_u/R_{d,max}$ ratio.
- Shear span = $L/2$. For copes with $c/D \leq 0.5$, or $0.5 < c/D \leq 0.8$ and $d_c/D \leq 0.05$, no reinforcement is required; for the remaining cases, Type A, B, or D reinforcement is sufficiently effective.

Based on the supplementary analysis performed in this study, some extra comments are noted as follows:

- It is recommended that the extension (e_x) of Type A reinforcement is taken as d_c, and this rule is also recommended for Types C and D reinforcements; no extension (e_y) is required for Type B reinforcement as the extension has no effect on the ultimate resistance; a full depth doubler plate is recommended for Type D reinforcement to maximise its efficacy.
- The proposed reinforcement details are also applicable to Cases 1 and 2 lateral bracing conditions, except that Type D reinforcement is not recommended for such cases.

It should be noted that the above recommended reinforcement details are based on the results of the parametric study of a beam section with a slender web (with the maximum d/t_w ratio among the available universal beams), a relatively small span-to-depth ratio (L/D = 10), and a limited range of cope details. Although the recommended reinforcement details may be safely applicable to other universal beams, engineers should be cautious when applying these recommendations for strengthening DCBs with other cope details.

6. Summary and conclusions

This paper presented a comprehensive numerical study on strength and behaviour of reinforced DCBs. An experimental investigation previously conducted by the authors and co-workers was employed to validate the numerical models. After showing good agreement between the numerical and test results, an extensive parametric study was carried out to examine the influence of varying reinforcing strategies on DCBs with a spectrum of cope details. Four reinforcement types were considered, namely, longitudinal web stiffener (Type A), combined longitudinal and vertical web stiffeners (Type B), vertical and double longitudinal web stiffeners (Type C), and doubler plate (Type D). The main findings based on the currently considered range of parameters are summarised as follows.

- The main failure modes of the unreinforced and reinforced models included local web buckling, web shear yielding, tensile fracture of the bottom cope corner, and web crippling, which are strongly dependent on the cope details and stiffener type. Local web buckling occurred only in the unreinforced models and the models with Type D reinforcement and concurrently a long cope. Web shear yielding tended to occur in the models with a short cope, i.e. $c \leq 0.2D$. Web crippling and tensile fracture of the bottom cope corner are two typical failure modes for the models with Type A reinforcement. Web crippling can be fully prevented by Type B reinforcement, and tensile fracture can be effectively delayed using Type C reinforcement. Web crippling is a common failure mode for the models with Type D reinforcement, especially for those with a deep cope.
- Compared with the unreinforced models, the presence of the reinforcement can increase the ultimate reaction to up to 4.5 times. The longer (or deeper) the cope, the more effective the reinforcement. Among the considered types of reinforcement, Type C is the most effective one in increasing the ultimate reaction. Types A and B reinforcements could increase the ultimate reaction to a similar extent, although different failure modes can be caused. A slightly less evident increase of ultimate reaction is achieved by Type D reinforcement.
- From a coped-section design point of view, conducting regular flexural yielding and shear yielding checking seems to be safe for either the unreinforced or Types A and B reinforced coped sections. For Type C reinforcement, a lower section utilisation efficiency is shown, and hence a reduction factor of 0.8 could be used for both $R_{y,co}$ and $R_{vy,co}$. For the case of Type D reinforcement, reduction factors of 0.8 and 0.5 may be conservatively used for $R_{y,co}$ and $R_{vy,co}$, respectively.
- From an overall steel beam design point of view, one may consider using reinforcements if the plastic moment capacity of the full beam section ($M_{p,b}$) or shear yielding capacity of the coped section cannot be achieved. A set of simple yet safe design

recommendations on the reinforcement details for DCBs is proposed, and the details are given in Section 5.

- Additional rules are also given in terms of geometric dimension of the reinforcements. Based on the limited numerical data, it is recommended that d_c is adopted for the extension (e_x) of Types A, C, and D reinforcements; no extension (e_y) is required for Type B reinforcement. A full depth doubler plate is recommended for Type D reinforcement to maximise its efficacy.
- Removing the lateral bracing of the beam top flange, but preventing the load application point from moving laterally (Case 1), could lead to comparable responses compared with the fully braced models. When the lateral bracing is completely removed (Case 2), the local web buckling resistance of the unreinforced models is significantly compromised, but Types A, C, and D reinforcements are highly effective in increasing the ultimate reaction. Type D reinforcement is not recommended for the Case 2 bracing condition, as the ultimate reaction can be decreased by 40%-50% when compared with the fully braced case.
- Types A through D reinforcement can all effectively increase the ultimate reaction, regardless of the connection rotational stiffness.

7. Acknowledgements

The work described in this paper is substantially supported by a grant from the Research Grants Council of the Hong Kong Special Administrative Region, China (Project No. PolyU 5288/13E). The partial support from the 'Program for Young Excellent Talents in Tongji University' to the first author is also gratefully acknowledged.

References

[1] Cheng JJ, Yura JA, Johnson CP. Design and behavior of coped beams. Ferguson Structural Engineering Laboratory Report No. 84-1, Department of Civil Engineering, University of Texas at Austin, July, 1984.

[2] Cheng JJR, Yura JA. Local web buckling of coped beams. Journal of Structural Engineering 1986;112(10):2314-31.

[3] Yam MCH, Lam ACC, Iu VP, Cheng JJR. The local web buckling strength of coped steel I-beam. Journal of Structural Engineering 2003;129(1):3-11.

[4] Fang C, Lam ACC, Yam MCH, Seak KS. Block shear strength of coped beams with single-sided bolted connection. Journal of Constructional Steel Research 2013;86:153-66.

[5] Wei F, Yam MCH, Chung KF, Grondin GY. Tests on block shear of coped beams with a welded end connection. Journal of Constructional Steel Research 2010;66(11):1398-410.

[6] Lam ACC, Fang C, Yam MCH, Wang W, Iu VP. Block shear strength and design of coped beams with double bolt-line connections. Engineering Structures 2015;100: 293-307

[7] Franchuk CR, Driver RG, Grondin GY. Experimental investigation of block shear failure in coped steel beams. Canadian Journal of Civil Engineering 2003;30(5):871-81.

[8] Topkaya C. Finite element modeling of block shear failure in coped steel beams. Journal of Constructional Steel Research 2007;63(4):544-53.

[9] Yam MCH, Cheng JJR. Fatigue strength of coped steel beams. Journal of Structural Engineering 1990; 116(9):2447-63.

[10] Roeder CW, MacRae G, Leland A, Rospo A. Extending the fatigue life of riveted coped stringer connections. Journal of Bridge Engineering 2005;10(1):69-76.

[11] Wen H, Mahmoud H. Ultra-low cycle fatigue demand on coped beam connections under vertical excitations. 8th International Conference on Behavior of Steel Structures in Seismic Areas, Shanghai, China, 2015.

[12] Ibrahim SA, Dessouki AK, El -Sa'eed SA. Lateral buckling behavior and strengthening techniques of coped steel I-beams. Journal of Constructional Steel Research 2015;108:11-22.

[13] Lam CC, Yam MCH, Iu VP, Cheng JJR. Design for lateral torsional buckling of coped I-beams. Journal of Constructional Steel Research 2000;54:423-43.

[14] Yam MCH, Fang C, Lam ACC, Cheng JJR. Local failures of coped steel beams – a state-of-the-art review. Journal of Constructional Steel Research 2014;102:217-32.

[15] American Institute of Steel Construction. Steel Construction Manual 14th Edition. One East Wacker Drive, Suite 700, Chicago, Illinois, 2011.

[16] The Steel Construction Institute and the British Constructional Steelwork Association Limited. Joints in Steel Construction: Simple Connections. Publication No. 212, UK, 2002.

[17] Aalberg A. Experimental and numerical parametric study on the capacity of coped beam ends. Journal of Constructional Steel Research 2015;113:146-55.

[18] Aalberg A. Design of aluminium beam ends with flange copes. Thin-Walled Structures 2015;94:593-602.

[19] Yam MCH, Lam ACC, Wei F, Chung KF. The local web buckling strength of stiffened coped steel-I-beam. International Journal of Steel Structures 2007;7(2):129-38.

[20] Yam MCH, Ma HW, Lam ACC, Chung KF. Experimental study of the strength and behaviour of reinforced coped beams. Journal of Constructional Steel Research 2011;67:1749-59.

[21] Yam MCH, Chung KF. A numerical study of the strength and behaviour of reinforced coped beams. Journal of Constructional Steel Research 2013;80:224-34.

[22] Fang C, Yam MCH, Lam ACC, Liu YH, Chung KF. Local web buckling of double-coped steel beam connections. Journal of Constructional Steel Research 2017;128:166-78.

[23] Yam MCH, Fang C, Lam ACC. Local web buckling mechanism and practical design of double-coped beam connections. Engineering Structures 2016;125:54-69.

[24] Lam ACC, Yam MCH, Fang C. Strength and behaviour of reinforced double-coped beams against local web buckling. Journal of Constructional Steel Research 2017; 138: 38-50.

[25] ABAQUS Analysis User's Manual. ABAQUS Standard, Version 6.12; 2012.

[26] Fang C, Wang W, He C, Chen YY. Self-centring behaviour of steel and steel-concrete composite connections equipped with NiTi SMA bolts. Engineering Structures 2017; 150: 390-408.

[27] EN 1993-1-5:2006, Eurocode 3: Design of Steel Structures – Part 1-5: Plated structural elements. European Committee for Standardization, Brussels, Belgium, 2006.

[28] EN 1993-1-1:2005, Eurocode 3: Design of Steel Structures – Part 1-1: General rules and rules for buildings. European Committee for Standardization, Brussels, Belgium, 2005.

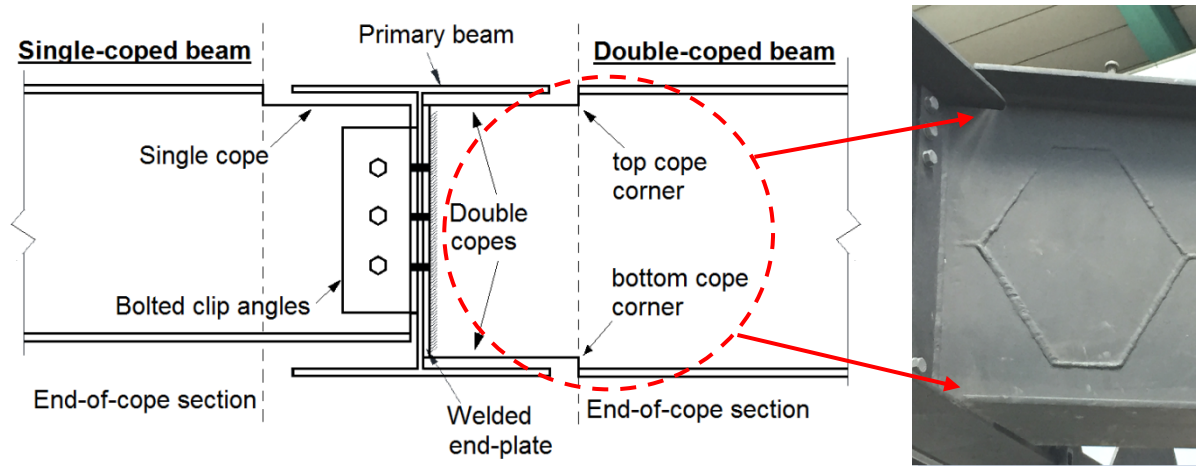

(a)

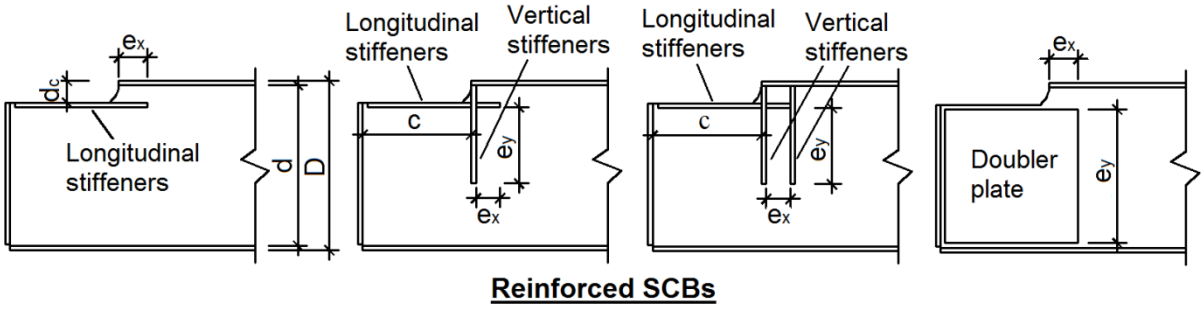

(b)

Fig. 1 Coped beam connections: a) practical coping details of steel beams, b) typical reinforcement for SCBs

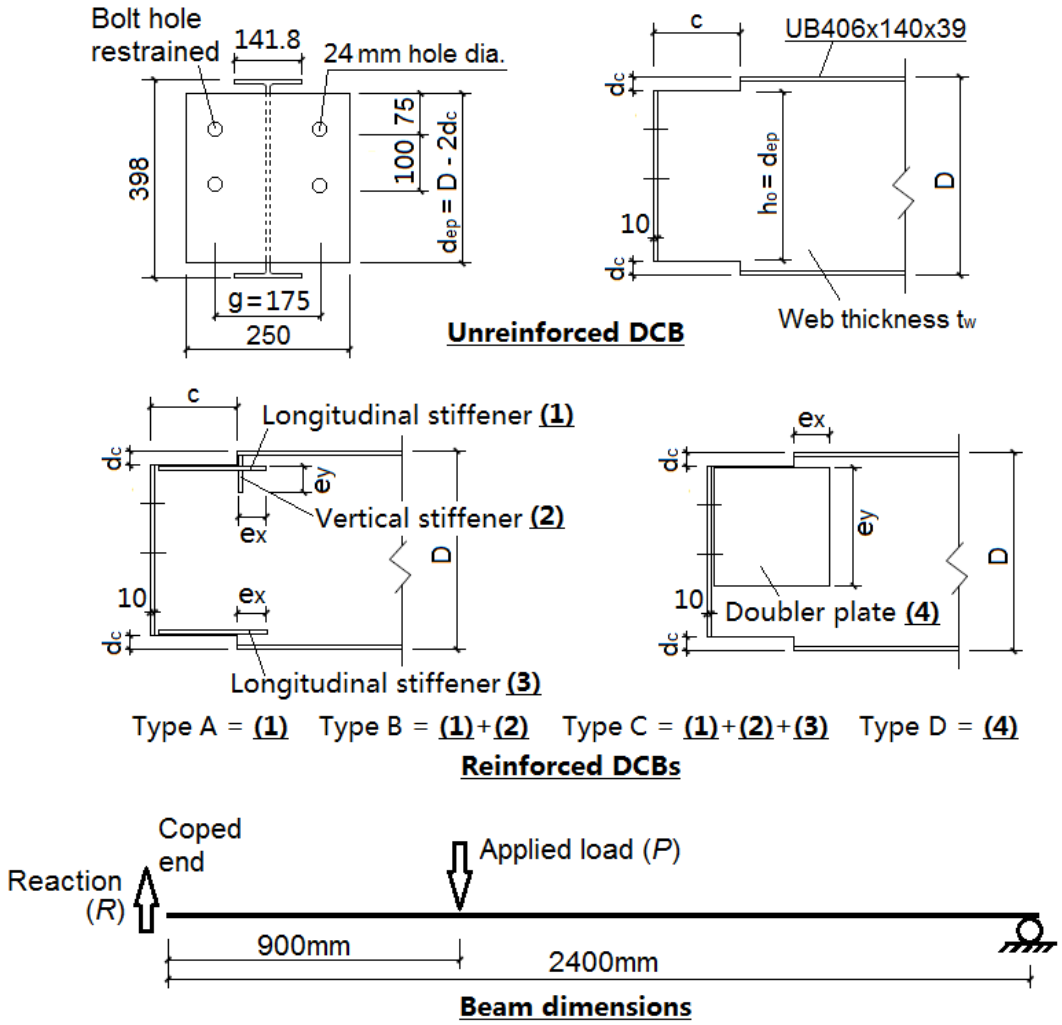

Fig. 2 Geometric configurations and key symbols of models for parametric study

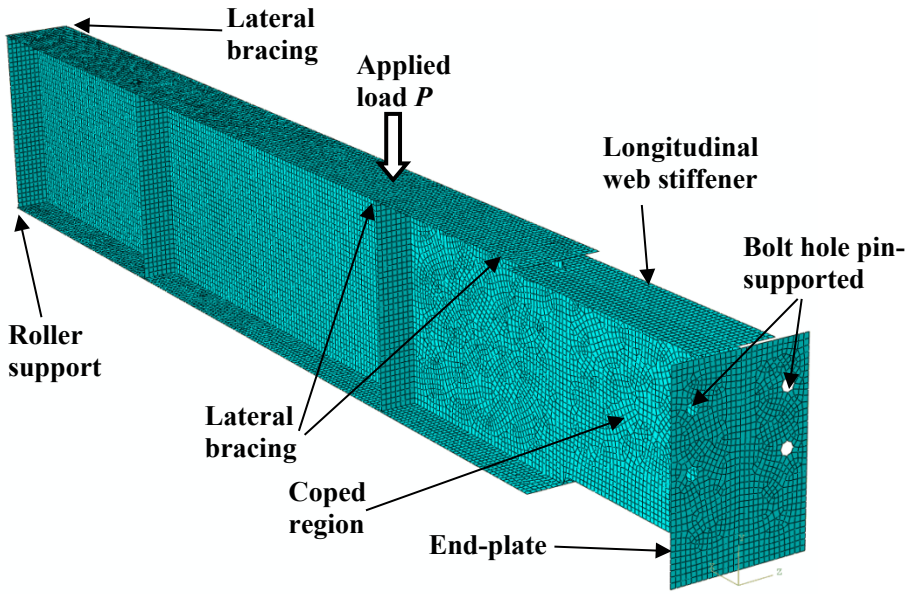

(a)

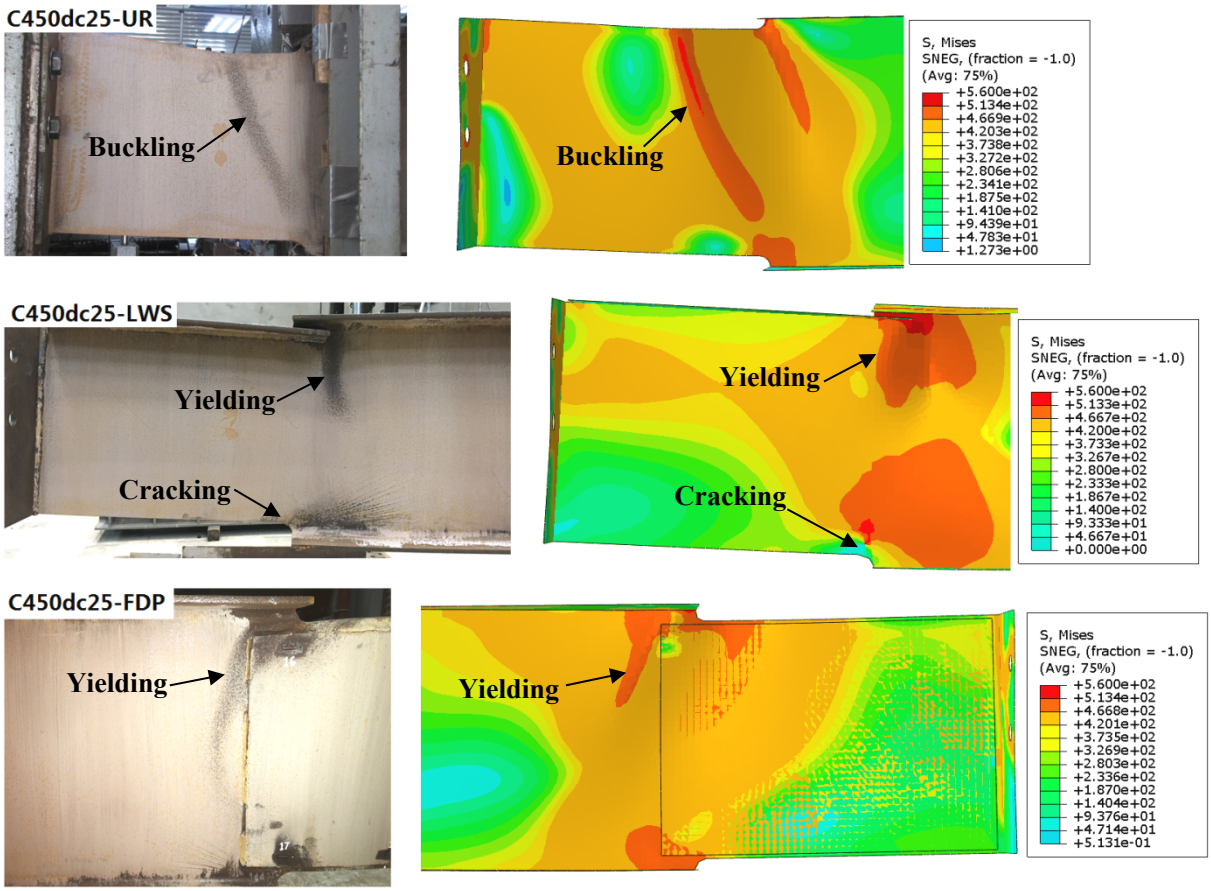

(b)

Fig. 3 FE models for validation: a) typical meshing scheme and boundary conditions, b) comparisons of failure modes

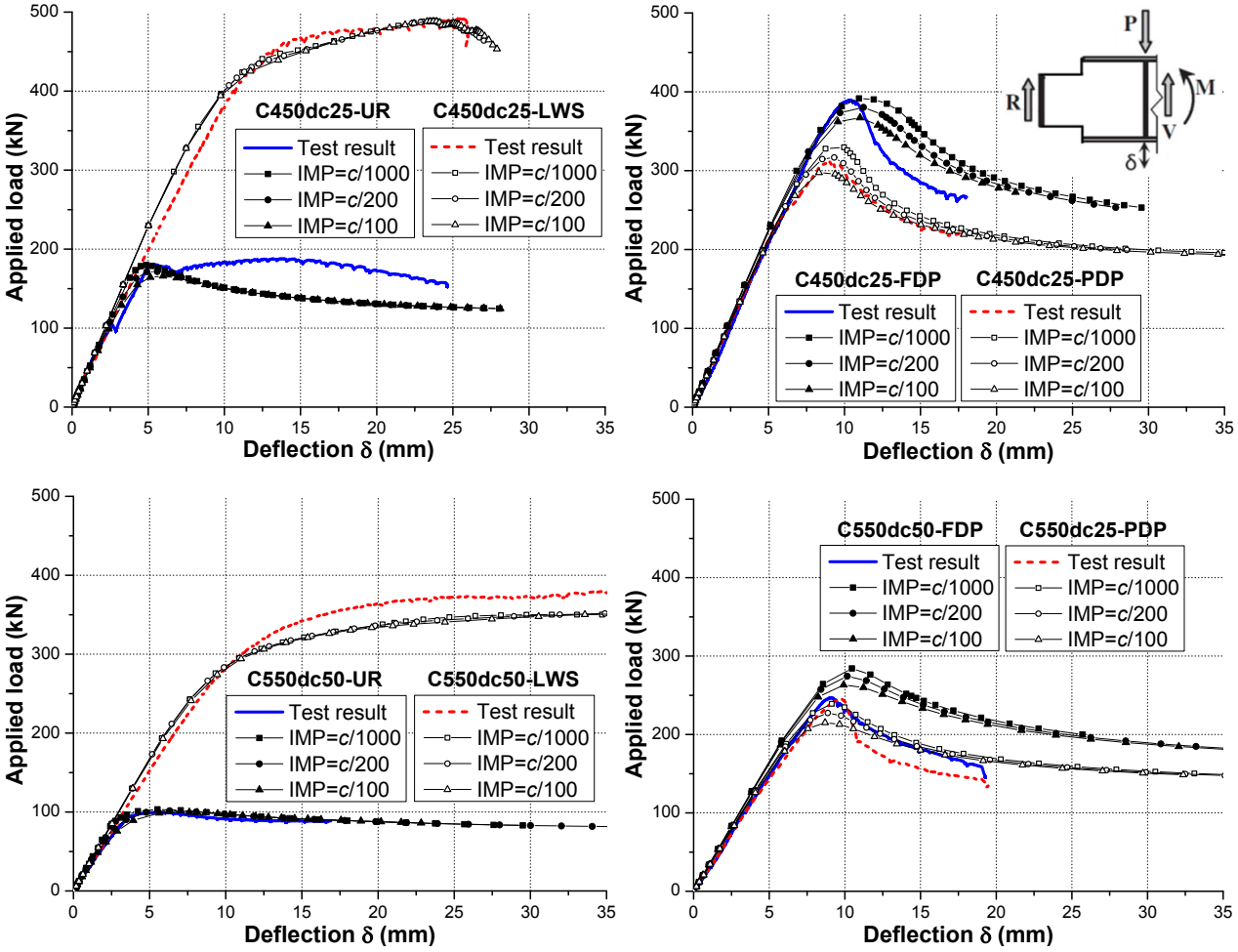

(a)

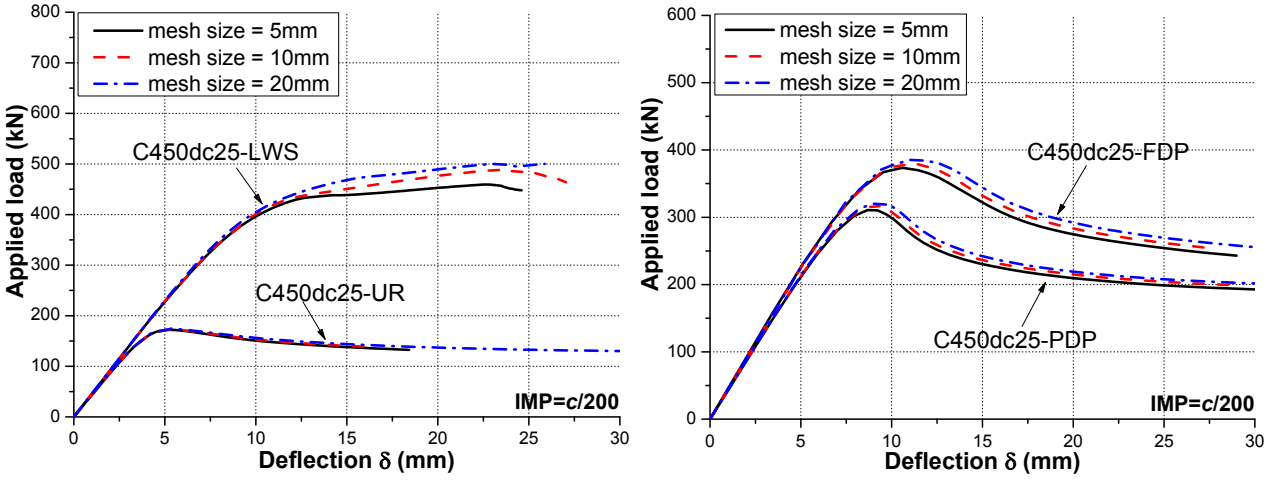

(b)

Fig. 4 Comparisons of load-deflection responses: a) imperfection sensitivity, b) mesh sensitivity

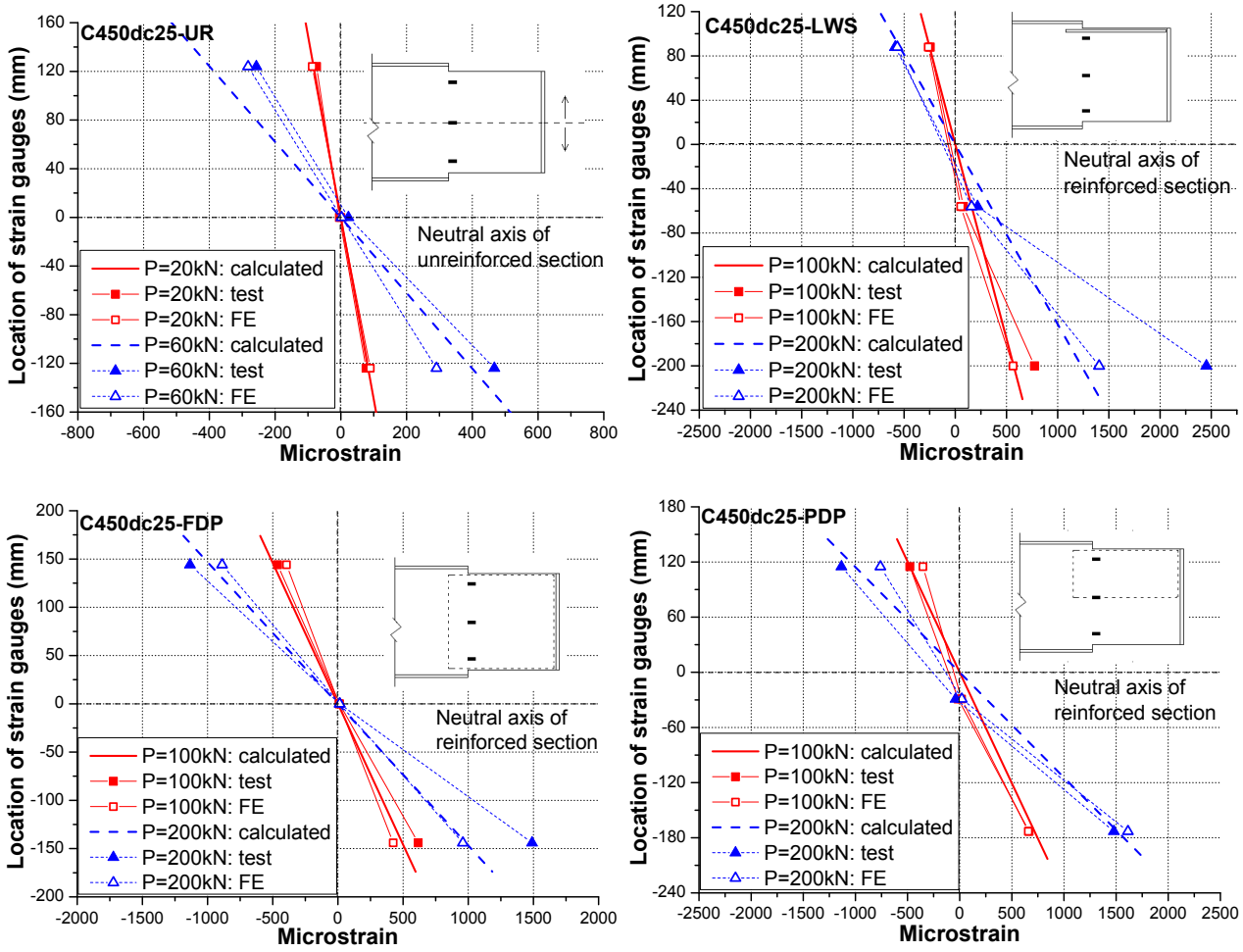

Fig. 5 Comparisons of strain responses

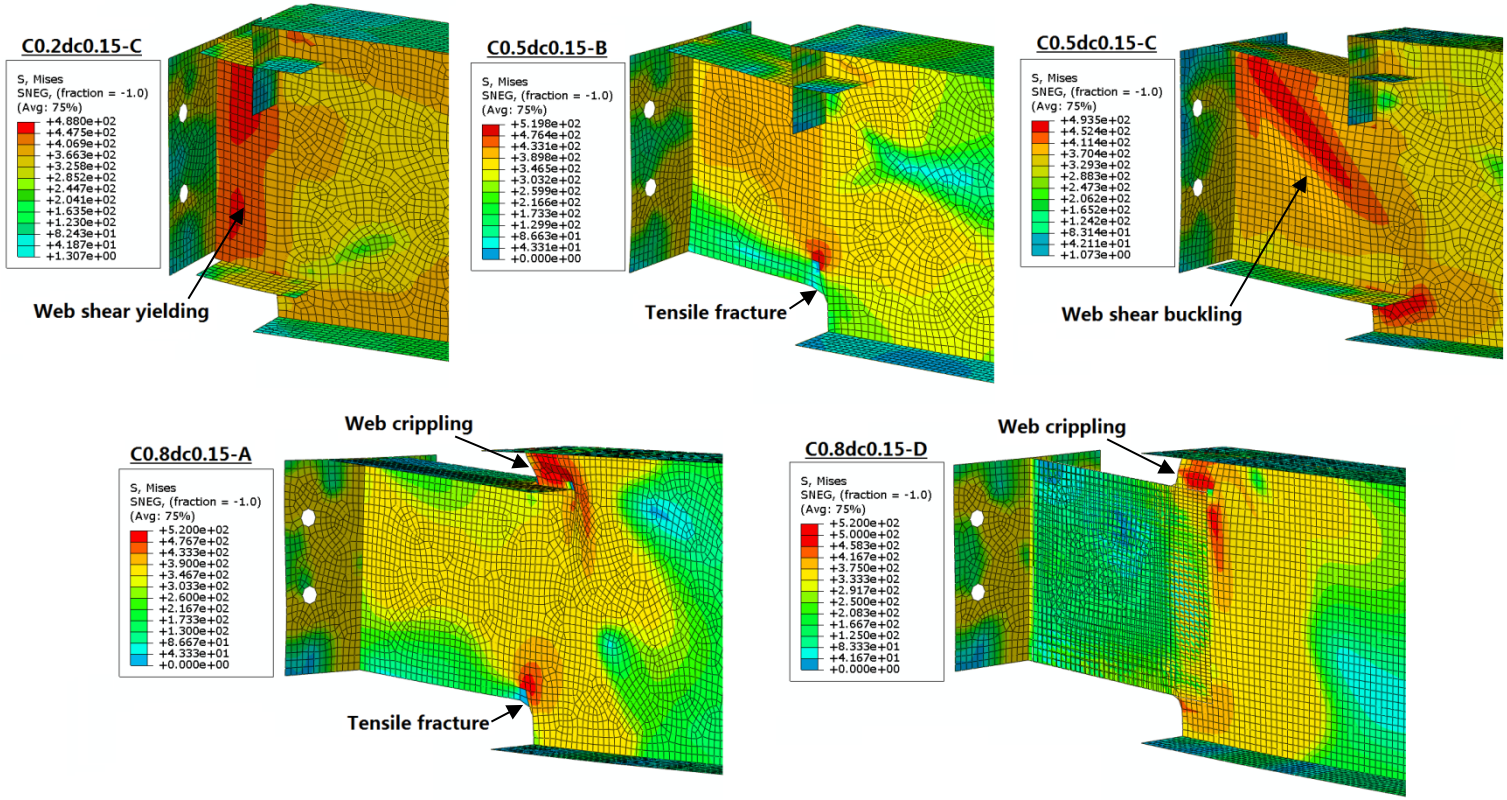

Fig. 6 Typical failure modes observed from parametric study

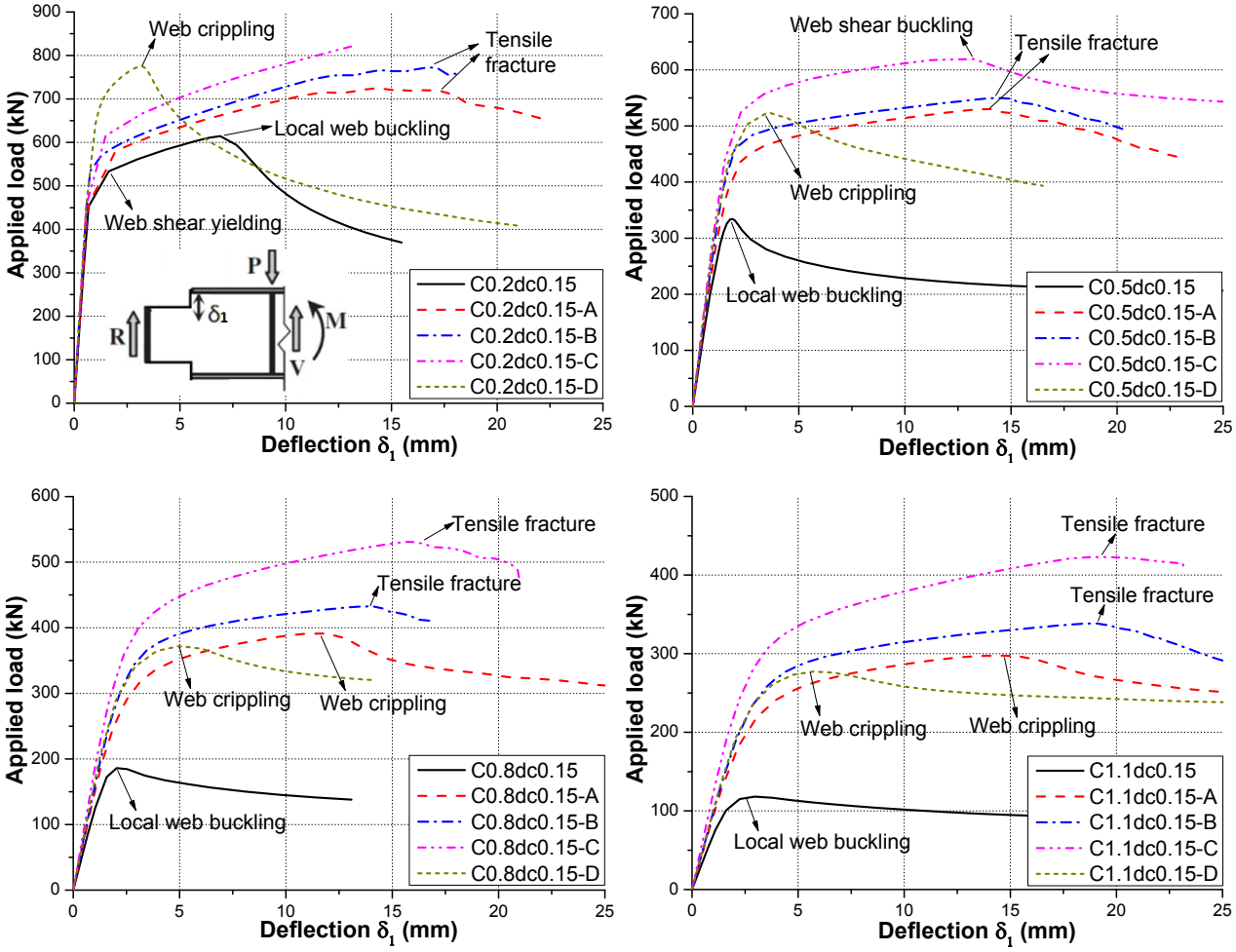

Fig. 7 Typical load-deflection responses obtained from parametric study

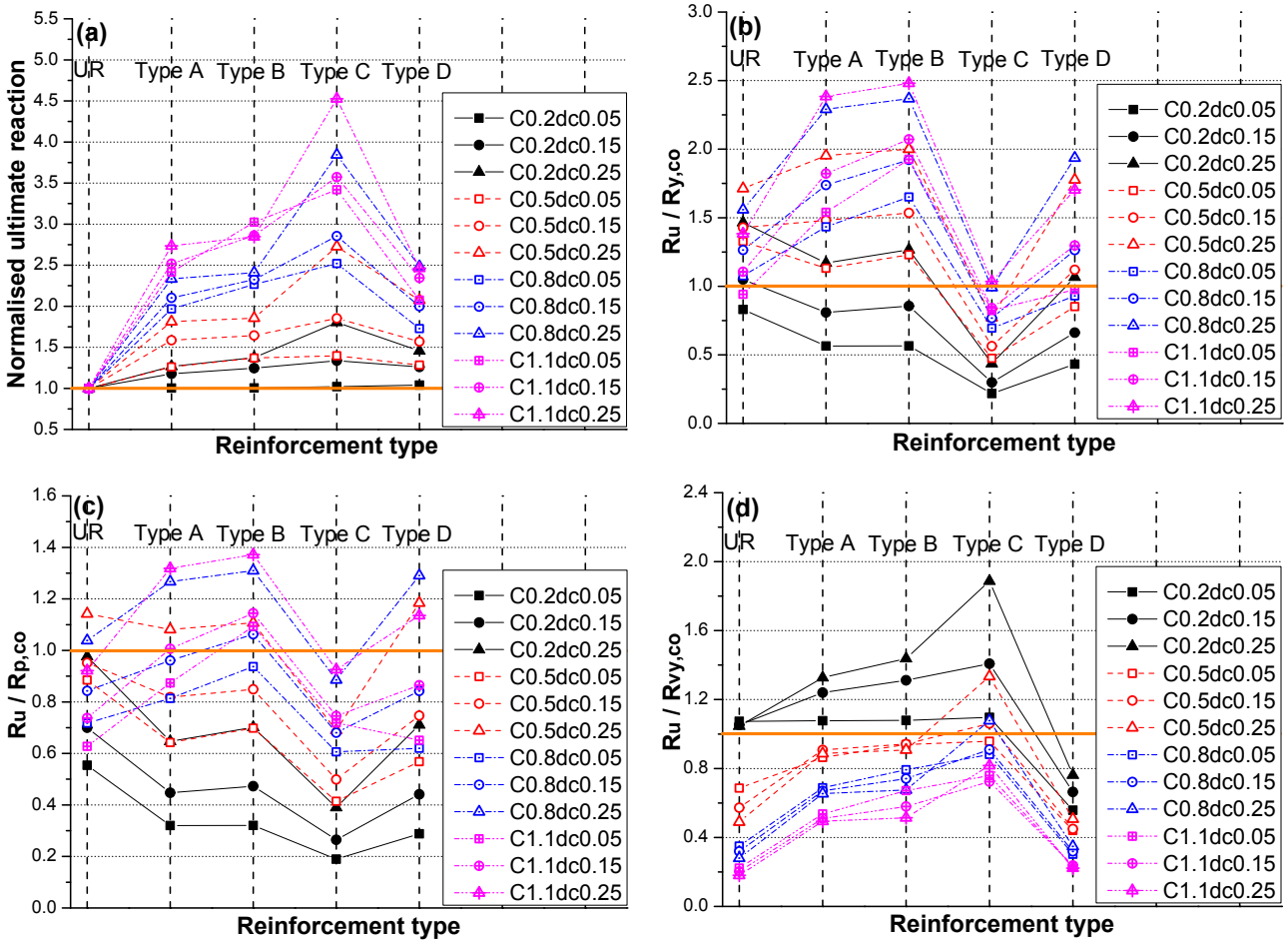

Fig. 8 Influence of varying parameters on ultimate reaction

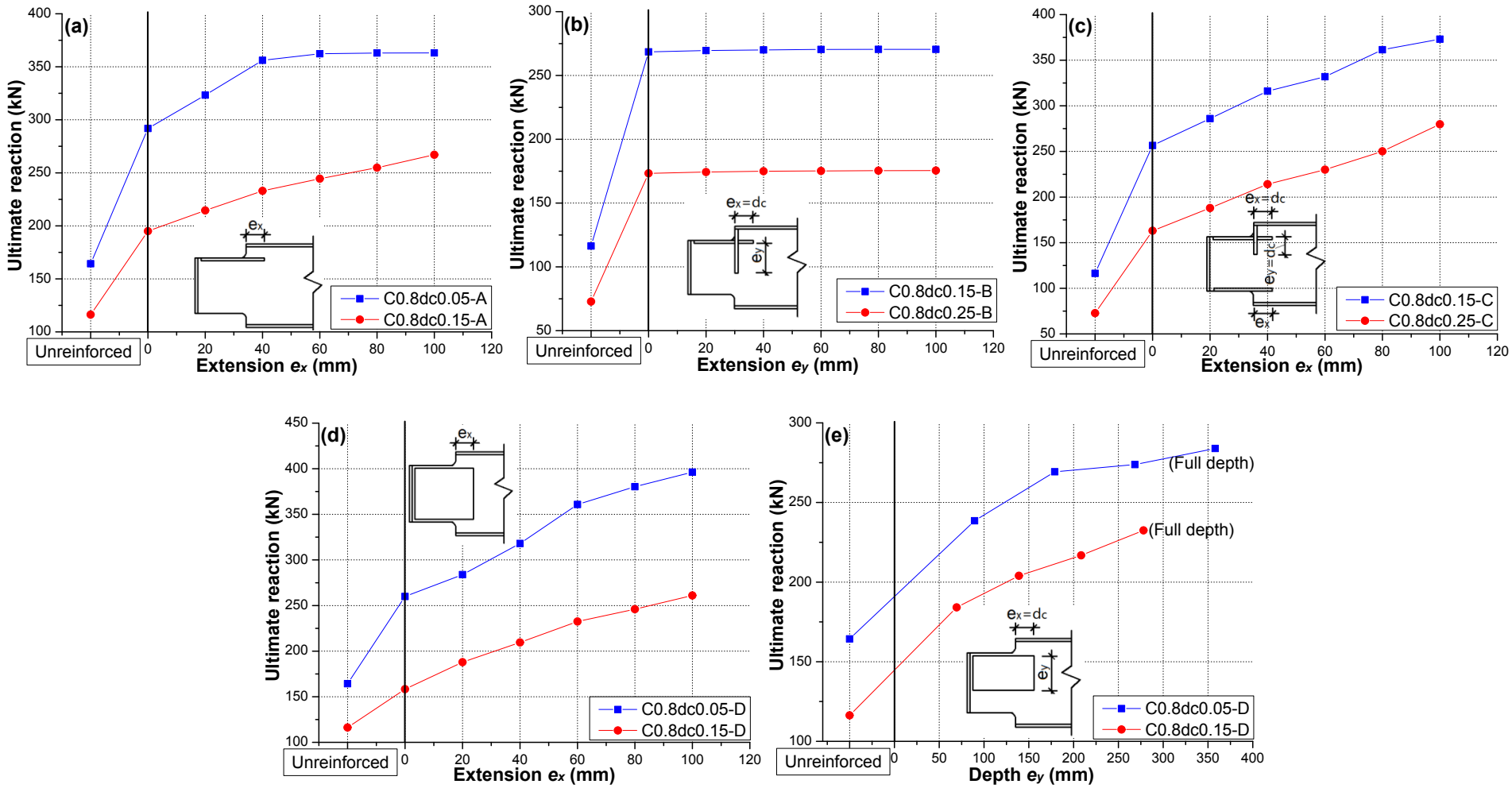

Fig. 9 Further discussions on influence of reinforcement extension

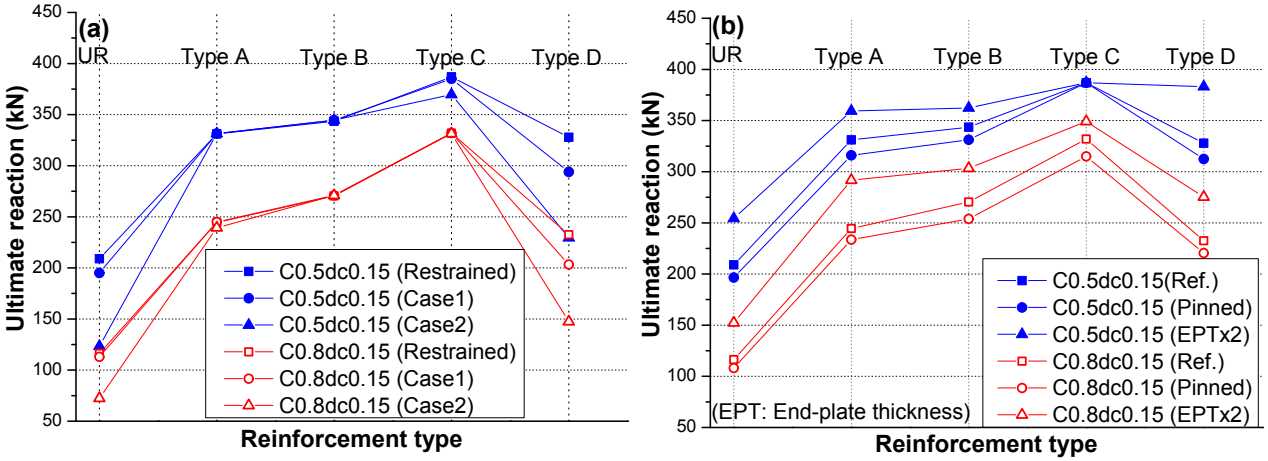

Fig. 10 Further discussions on influences of lateral bracing and connection stiffness

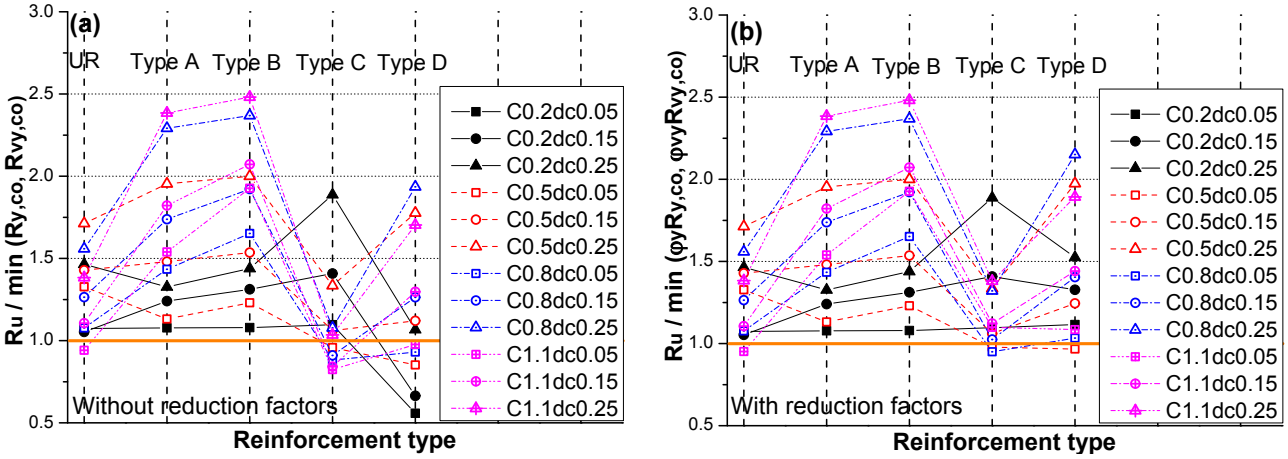

Fig. 11 Yielding design of DCB sections

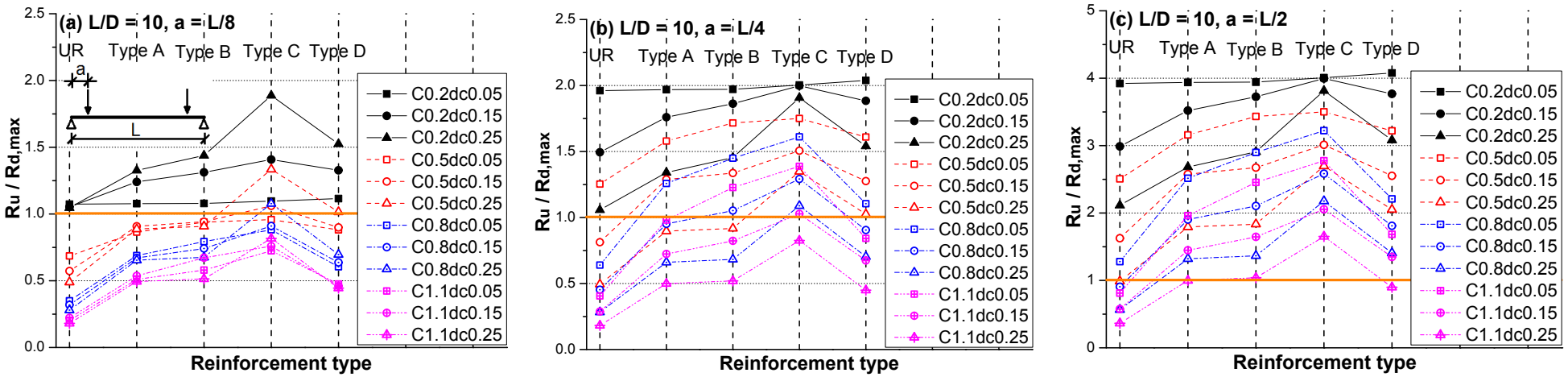

Fig. 12 Effectiveness of reinforcement details for a typical steel beam

Table 1 Key information of test specimens and comparisons against FE predictions

Test specimens	Cope length c (mm)	Cope depth d_c (mm)	Web thickness t_w (mm)	Stiffener or doubler plate thickness t_s or t_d (mm)	Ultimate load P_{test} (kN)	Ultimate reaction R_{test} (kN)	Failure mode	Ultimate load by FE prediction P_{FE} (kN) [P_{FE}/P_{test}]		
								IMP=c/1000	IMP=c/200	IMP=c/100
C450dc25-UR	450	24	6.12	-	180.7	114.5	LWB	179.8[1.00]	171.5[0.95]	165.9[0.92]
C450dc25-LWS	450	26	6.19	8.29	481.9	306.0	FCC	489.1[1.01]	488.5[1.01]	488.3[1.01]
C450dc25-FDP	450	26	6.22	6.28	385.7	241.8	LWB	391.6[1.02]	380.3[0.99]	367.1[0.95]
C450dc25-PDP	450	26	6.13	6.18	306.9	192.6	LWB	329.7[1.07]	316.6[1.03]	297.5[0.97]
C550dc50-UR	550	49	6.19	-	98.7	62.1	LWB	103.3[1.05]	101.6[1.03]	99.7[1.01]
C550dc50-LWS	550	52	6.14	8.33	379.1	239.8	FCC	350.8[0.93]	350.5[0.92]	350.1[0.92]
C550dc50-FDP	549	52	6.26	6.17	244.6	155.7	LWB	284.2[1.16]	274.3[1.12]	263.2[1.08]
C550dc50-PDP	550	51	6.26	6.15	243.9	154.4	LWB	239.0[0.98]	227.5[0.93]	215.0[0.88]
							Mean P_{FE}/P_{test}	**1.03**	**1.00**	**0.97**
							CoV	**0.069**	**0.065**	**0.065**

Note 1: UR = Unreinforced, LWS = Longitudinal web stiffener, FDP = Full-depth doubler plate, PDP = Partial-depth doubler plate, IMP = Initial imperfection amplitude, LWB = Local web buckling, FCC = Fracture of cope corner.
Note 2: Measured values are given in the table.

Table 2 Key material properties from coupon tests

Test specimens	Locations	Yield strength f_y (MPa)	Ultimate strength f_u (MPa)	Young's modulus E (GPa)	Strain at fracture ε_f (%)
C450dc25-UR	Web	460	596	200	16.0
	Flange	358	510	197	17.5
C450dc25-LWS	Web	461	592	203	16.2
	Flange	418	554	206	15.9
C450dc25-FDP	Web	461	592	203	16.2
	Flange	418	554	206	15.9
C450dc25-PDP	Web	432	586	201	14.9
	Flange	372	524	208	14.5
C550dc50-UR	Web	475	601	202	15.4
	Flange	402	563	203	15.7
C550dc50-LWS	Web	432	586	201	14.9
	Flange	372	524	208	14.5
C550dc50-FDP	Web	434	575	197	16.5
	Flange	417	570	201	15.9
C550dc50-PDP	Web	434	575	197	16.5
	Flange	417	570	201	15.9

Table 3 Considered parameter matrix

Varying parameters	Range	Details
c/D ratio	0.2, 0.5, 0.8, 1.1	c = 80 mm, 200 mm, 318 mm, 438 mm
d_c/D ratio	0.05, 0.15, 0.25	d_c = 20 mm, 60 mm, 100 mm
Reinforcement type	UR, Type A, Type B, Type C, Type D	Unreinforced (UR), longitudinal web stiffener (Type A), combined longitudinal and vertical web stiffeners (Type B), vertical and double longitudinal web stiffeners (Type C), and full-depth doubler plate (Type D),